Available online at www.sciencedirect.com

ScienceDirect

Procedia Engineering 148 (2016) 86 – 92

Procedia Engineering

www.elsevier.com/locate/procedia

4th International Conference on Process Engineering and Advanced Materials

Surface Modification of AMH-3 for Development of Mixed Matrix Membranes

Elaine Chong Nyuk Tzi[a] and Oh Pei Ching[a,*]

[a]*Chemical Engineering Department, Universiti Teknologi PETRONAS, 32610 Bandar Seri Iskandar, Perak, Malaysia*

Abstract

AMH-3 layered silicate is an attractive material for gas separation applications due to its 3D structure with crystallographic pore size of 3.4 Å. Nevertheless, AMH-3 is strongly hydrophilic due to the presence of cations between the silicate layers. Therefore, surface modification of AMH-3 is necessary in order to enhance its compatibility with hydrophobic polymer matrix of membranes. In this study, AMH-3 layered silicate was synthesized via hydrothermal synthesis method and functionalized with octyl(methyl)dimethyoxysilane to enhance its hydrophobicity, thereby improve adhesion and dispersion in mixed matrix membrane (MMM). The as-synthesized and functionalized AMH-3 were characterized with analytical tools such as FT-IR, XRD, SAP and contact angle. Functionalized AMH-3 showed higher surface area but reduced pore size. It also exhibited improved hydrophobicity compared to as-synthesized AMH-3. Flat sheet PSf/AMH-3 membranes were subsequently prepared by dry/wet phase inversion technique with varying AMH-3 loadings (1, 3 and 5 wt.%). As apparent from the thermogravimetric analysis, as-synthesized and functionalized AMH-3 showed no significant effect on the thermal stability and decomposition temperatures of the resultant MMMs. The synthesized membranes exhibited similar surface and cross-sectional morphologies with good distribution and dispersion of inorganic filler. Functionalized AMH-3 showed improved hydrophobicity, which results in enhanced compatibility and adhesion with the hydrophobic PSf polymer matrix.

Peer-review under responsibility of the organizing committee of ICPEAM 2016

Keywords: AMH-3; Layered Silicate; Functionalization; Mixed Matrix Membrane

1. Introduction

Mixed matrix membrane (MMM) is receiving widespread attention due to its potential of improving gas separation performance and offer enhanced mechanical properties over conventional polymeric membranes [1]. However, poor interfacial contact between polymer and inorganic filler often results in the formation of voids, therefore affects the membranes' performance [2]. Generally, polymeric matrix possesses strong hydrophobic characteristics whereas inorganic fillers such as AMH-3 layered silicate is strongly hydrophilic due to the presence of interlayer cations [3]. Therefore, modification of the layered silicate is often necessary in order to enhance the compatibility between the inorganic filler with the polymeric matrix.

AMH-3 is a 3-dimensional microporous layered material with eight membered ring (8 MR) pores, built of silicate layers with sodium cation, strontium cation and water molecules taking up the interlayer spaces. The unit cell formula of AMH-3 is $Na_8Sr_8Si_{32}O_{76}{\cdot}16H_2O$. The silicate layers contain plurality of tetrahedral SiO_4 units and channels formed by eight membered rings of ≡Si-O-Si≡ units and contributes to the porosity of the material. A plurality of cations including sodium ions and

* Corresponding author. Tel.: +605-368 7568; Fax: +605-365 6176.
E-mail address: peiching.oh@petronas.com.my

Peer-review under responsibility of the organizing committee of ICPEAM 2016
doi:10.1016/j.proeng.2016.06.443

strontium ions are located between the layers [3]. On top of its excellent acid and thermal stability, its 3.4 Å crystallographic pore size is particularly useful for gas separations such as CO_2/CH_4 and H_2/N_2 [4]. Choi, et al. [5] reported the fabrication of MMM by dispersing AMH-3 into polybenzimidazole (PBI) matrix, which showed a twofold enhancement of selectivity for H_2/CO_2 separation. On the other hand, Kim, et al. [6] delaminated swollen AMH-3 into flakes and incorporated it into cellulose acetate matrix. Enhancement in the CO_2 permeability and CO_2/CH_4 gas separation performance were observed.

Although layered silicate materials showed excellent properties for MMMs fabrication, their hydrophilicity results in poor interfacial interactions with non-polar polymers [7]. Therefore, the layered silicate materials require surface modification to enhance their miscibility with the polymer before being embedded into the matrix. Structural modification such as swelling is often performed to enhance the interlayer spacing. Takahashi and Kuroda [8] introduced different covalent modification methods for the layered silicates. The modification can be carried out with different silylation reagents such as amino, thiol, and alkyl groups. The properties of silanol groups on AMH-3 surface and charge-balancing cations in the interlayer spaces rendered the conventional procedures for clay swelling ineffective [6]. Subsequently, Choi, et al. [9] introduced the AMH-3 swelling process by proton exchange using amino acid followed by sequential intercalation with amine molecules.

Polysulfone (PSf) is generally used as the polymer phase for MMM fabrication as it exhibits good mechanical strength, resistance and chemical stability as well as being cost effective [10]. It also demonstrates high permeability and good selectivity in CO_2/CH_4 gas separation [11]. Besides polymer and inorganic fillers selection, 'priming' technique is suggested to enhance the compatibility of the inorganic filler with the polymer [12]. Typically, 5−10 wt.-% of the total polymer required to form a membrane is added into the dope solution of inorganic fillers and solvent. Priming of inorganic particles before dispersing in the polymer matrix minimizes interface stress and improves interaction between the primed inorganic particles and polymer matrix. Subsequently, the agglomeration of inorganic particles and formation of defective interfaces can be minimized [13].

Formation of macrovoids is an unfavourable defect in solution-cast membranes as it jeopardizes the mechanical integrity of a polymeric membrane [14]. Peng, et al. [15] suggested that the formation of macrovoids can be suppressed at a critical polymer concentration. Therefore, viscometric test is carried out to determine the optimum PSf concentration for MMM fabrication.

This paper reports the synthesis and surface modification of AMH-3 layered silicate by silane condensation. The as-synthesized and functionalized AMH-3 were incorporated into PSf matrix for fabrication of MMM. The structure of the AMH-3 and resultant membranes were characterized using various analytical tools.

2. Experimental

2.1. Determination of critical polysulfone viscosity

Dried polysulfone (PSf) pellets of 10, 15, 20, 25, 28 wt.-%, purchased from Sigma-Aldrich (M.W. 35,000) were slowly added into the corresponding wt.-% of *N*-methyl-2-pyrrolidone (NMP) supplied by Merck, while stirring at 50°C. Heating was stopped after complete dissolution of PSf and the mixture was continuously stirred for another 20 hours. The viscosity of each PSf/NMP solution was determined using Fungilab Rotational Viscometer (Model Alpha L) at 30 rpm. The viscosity curve was plotted based on the viscometric readings. The critical polymer concentration of PSf/NMP binary mixture was obtained from the intersection point of the extrapolated lines from the two linear parts of the viscosity curve.

2.2. Synthesis of AMH-3 layered silicate

AMH-3 layered silicate was prepared by hydrothermal synthesis for 3 days at 200°C. 0.704g sodium hydroxide (99%, Merck) was added into 28.24g of deionized water. 1.502g of strontium chloride hexahydrate (99%, Aldrich) was then added into the solution while heating at 80°C. After 30 minutes of stirring, 6.26g sodium silicate (27% SiO_2, 14% NaOH, Aldrich) was added drop-wise to obtain a white, cloudy solution. After another 30 minutes of stirring, 2.17g titanium (III) chloride solution (20% w/w solution in 2N HCl, Acros Organics) was added drop-wise to produce a dark purple, cloudy solution. The solution was stirred vigorously for 60 minutes before pouring into a Teflon-lined stainless steel hydrothermal reactor. The hydrothermal synthesis was conducted for 3 days at 200°C. Subsequently, deionized water was added into the suspension and placed in an ultrasonic bath for 60 minutes. The suspension was decanted and the sediment was washed with deionized water. The suspension was allowed to settle for 5 minutes. The washing was repeated 5 times before the precipitate was filtered. AMH-3 solids were obtained after overnight drying in vacuum oven at 80°C.

2.3. Proton exchange and swelling of AMH-3

0.776g of DL-histidine (99%, Aldrich) was dissolved in 25ml deionized water at 60°C under vigorous stirring until a clear solution was obtained. The solution was cooled to room temperature with continuous stirring. A few drops of concentrated hydrochloric acid (37%, Merck) were added until the pH of the solution was adjusted to pH 6.0. Proton exchange was performed by adding 0.2g of AMH-3 into the buffer solution and stirred vigorously. The swelling agent solution was prepared by dissolving 2.061g of dodecylamine (98%, Aldrich) in 50ml of deionized water at 60°C and continuously stirred for 30 minutes. After 60 minutes of proton exchange, the swelling agent solution was added drop-wise and stirred for 12 hours. The swollen AMH-3 was washed with deionized water and centrifuged for 3 times. The product was then air dried at room temperature.

2.4. Functionalization of AMH-3

0.2g of swollen AMH-3 was dried overnight at 80°C. The swollen AMH-3 was added to 4g anhydrous toluene (Merck) and 0.4g of octyl(methyl)dimethoxysilane (95%, Aldrich) mixture solution. The mixture was refluxed for 16 hours. Pure toluene was added into the reaction vessel and agitated. The upper layer of the suspension was decanted after sedimentation of AMH-3 particles. Washing was repeated with toluene for 3 times. The product was then dried overnight at 60°C.

2.5. Fabrication of mixed matrix membrane (MMM)

As-synthesized and functionalized AMH-3 at various concentrations (0, 1, 3, 5 wt.-%) were dissolved in NMP solvent. The solution was placed in an ultrasonic bath for 30 minutes to break the aggregates of AMH-3. Approximately 10% of the required PSf was added into the solution and stirred for 6 hours. The remaining PSf pellets were added into the solution and stirred for another 12 hours. The solution was sonicated for 30 minutes to remove trapped bubbles. The solution was poured on a glass plate and cast using a casting knife. The membrane film was left to evaporate for 60 seconds before immersing it into distilled water coagulation bath for 24 hours. The membrane was finally air dried at room temperature for 48 hours.

2.6. Characterization

Fourier Transform Infrared Spectroscopy (FT-IR) spectra were obtained using Pelkin Elmer Spectrum One. X-ray Diffraction (XRD) patterns were obtained with Bruker AXS D8 Advance. N_2 isotherm and BET surface area were measured with Micromeritics ASAP 2020. Scanning electron microscopy (SEM) images and Energy Dispersive X-ray (EDX) analysis were obtained using Hitachi TM 3030 operating at accelerating voltage of 15 kV. Thermal gravimetric analysis (TGA) was carried out using a Perkin Elmer STA 6000 system heated from 30ºC to 600ºC with N_2 purging at a heating rate of 10ºC/min. The contact angle between water and membrane film was measured by using ramé-hart Model 290 goniometer.

3. Results and Discussion

3.1. Determination of critical polysulfone concentration

The viscosity curve of PSf/NMP is shown in Figure 1. A sharp slope is observed as the PSf concentration increases above 20 wt.-%. According to Chung, et al. [16], the critical concentration for a polymer/solvent binary system can be determined by the intersection of extrapolation lines of the two linear parts of the viscosity curve. The critical concentration of PSf/NMP dope solution is determined to be 23 wt.-%. The critical concentration exists due to the close intermolecular interactions and chain entanglements of polymer [15]. At a concentration lower than the critical value, polymer chains exhibit loose packing which allows the non-solvent to infiltrate into the chain spaces of polymer solution and subsequently form macrovoids. Beyond the critical polymer concentration, the polymer chains form entanglements as they become closely packed. The entangled network structure strengthens the membrane to handle shrinkage stress, inhibits access of the non-solvent, and thus suppresses defects such as macrovoids formation [15]. Thereafter, MMMs were cast using 23 wt.-% PSf while varying the AMH-3 loadings, respectively.

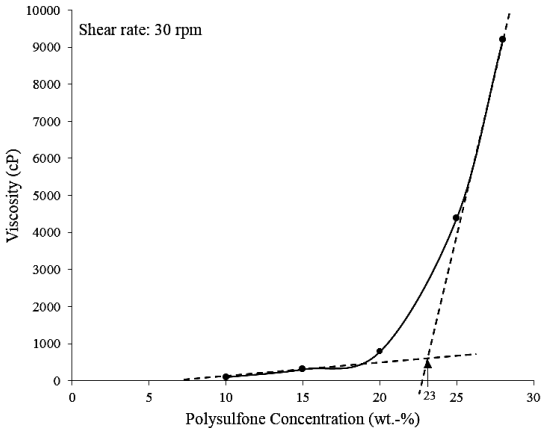

Fig. 1. Viscosity curve of PSf/NMP dope solution

3.2. Characterization of as-synthesized and functionalized AMH-3

AMH-3 which was prepared by hydrothermal synthesis underwent proton exchange and swelling, before functionalization using silane group. Figure 2 shows the FT-IR spectra of the as-synthesized and functionalized AMH-3. Vibrational bands measured between 1300 and 400 cm^{-1} represent the internal Si-O linkages of the SiO_4 tetrahedral and the external linkages connected to other tetrahedral or chemical groups [9] [17]. On the other hand, the spectra in the range of 4000 to 2500 cm^{-1} provide information on the interlayer hydroxyls and can be used to distinguish different silanol proton species [18]. Layer structure of as-synthesized AMH-3 is formed by single four-membered rings (S4R) that consists of four silicon atoms (Si1, Si2, Si3, and Si4) [4]. The S4Rs are designated to the bands between 650 and 500 cm^{-1}, whereas the bands between 1150 and 1050 cm^{-1} are ascribed to the external linkages of Si-O asymmetric stretch [17]. Bands shown around 3600 cm^{-1} can be attributed to the hydroxyl groups of the lattice water which is situated in the interlayer gallery of the original framework [4]. The FT-IR spectra for as-synthesized AMH-3 corresponds to the band assignments obtained from literature, indicating the successful synthesis of AMH-3.

Structural changes is observed in FT-IR spectra after the functionalization of AMH-3 layered silicate. The absorption bands between 500 and 420 cm^{-1} corresponding to Si-O bend are replaced by only a single band after functionalization. The absorption bands between 650 and 500 cm^{-1} corresponding to S4Rs become insignificant after functionalization. Furthermore, functionalized AMH-3 shows absorption bands of lower intensity in the range of 720 and 650 cm^{-1}, indicating the decrease of framework crystallinity [9]. The absorption band around 3600 cm^{-1} for lattice water is no longer noticeable after the functionalization of AMH-3. Also, the functionalized AMH-3 shows absorption bands between 3000 and 2850 cm^{-1}, similar to swollen AMH-3 which are suggested to be the C–H stretching of CH_3 and $–CH_2–$ aliphatic chains. The FT-IR spectra of functionalized AMH-3 showed good agreement with the spectra of swollen AMH-3 in the paper by Choi, et al. [9].

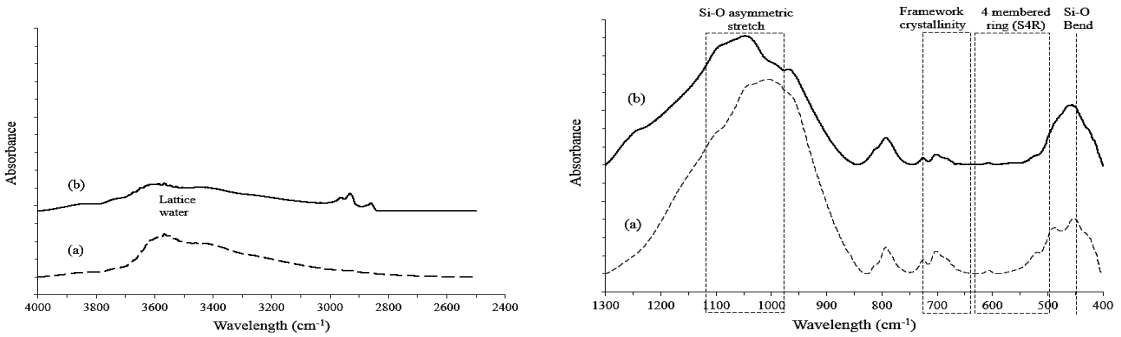

Fig. 2. FT-IR spectra of (a) as-synthesized AMH-3 and (b) functionalized AMH-3 at wavelengths 4000 to 2500 cm^{-1} and 1300 to 400 cm^{-1}

Figure 3 shows the XRD patterns of as-synthesized AMH-3 and functionalized AMH-3. The characteristic peaks of as-synthesized AMH-3 in Fig. 3a indicate the crystalline structure of AMH-3 layered silicate. According to Choi, et al. [9], the AMH-3 layered silicate becomes more amorphous after the proton exchange step. Furthermore, the amorphous structure of the proton-exchanged AMH-3 is maintained throughout the swelling and functionalization steps [19]. Consistent with the FT-IR results, the XRD pattern of functionalized AMH-3 in Fig. 3b illustrates the decrease in crystallinity.

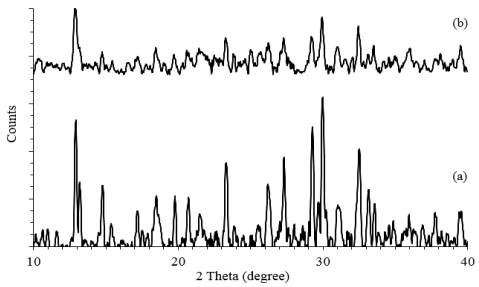

Fig. 3. XRD pattern of (a) as-synthesized and (b) functionalized AMH-3

The as-synthesized and functionalized AMH-3 show adsorption characteristics of macroporous materials [20]. The low porosity of the material is possibly caused by the small aperture of the 8 membered ring and the blocking of pore by intra and interlayer cations [9]. The specific surface areas are determined using the Brunauer–Emmett–Teller (BET) technique and the pore size averages are calculated using the Barrett–Joyner–Halenda (BJH) method. The specific surface area and pore size of as-synthesized AMH-3 are 18.75 m^2/g and 145.27 Å, respectively. The functionalized AMH-3 showed a BET surface area of 37.16 m^2/g and pore size of 63.35 Å. The increase in surface area after functionalization is most likely due to the attachment of alkoxysilane to the layer of the inorganic filler [19]. On the other hand, the decrease in pore size of functionalized AMH-3 might be caused by the pore space of the layered silicate being occupied by the bonded alkyl phase [21].

3.3. Characterization of mixed matrix membrane (MMM)

SEM characterization is aimed to determine the extent of adhesion and dispersion of AMH-3 in PSf matrix. Figure 4 illustrates the surface and cross-sectional morphologies of MMM with different loadings of as-synthesized AMH-3. The uniform scattering of white particles on the surface of MMM implies good distribution and dispersion of AMH-3 in Fig. 4a, 4b and 4c. The particles tend to agglomerate as the filler loading increases, due to the increase contact of the particles. At 5 wt.-% of AMH-3 loading in MMM, large white agglomerates of the fillers are observed on the surface morphology, indicating particle agglomeration. Figure 4d, 4e and 4f show the cross-sectional images of MMM at increasing loading of AMH-3. It is observed that there are minimal formation of voids surrounding the AMH-3 fillers.

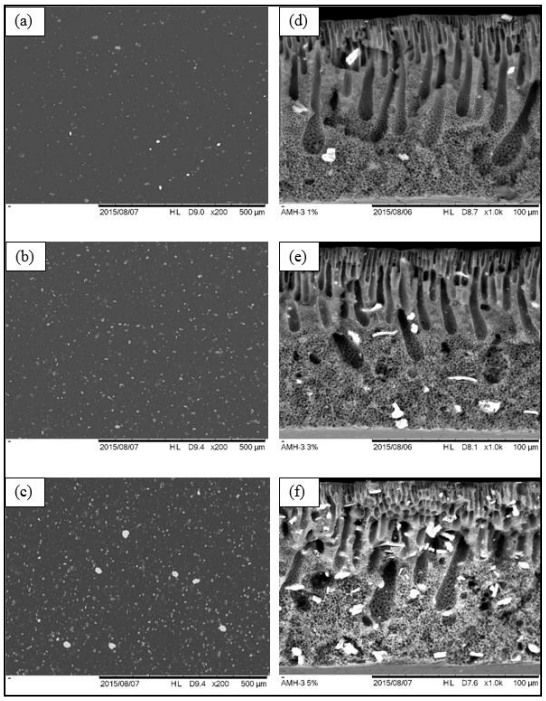

Fig. 4. Surface morphology of MMM with different loadings of AMH-3 at (a) 1 wt.-%, (b) 3 wt.-%, and (c) 5 wt.-%; and cross-section morphology with (d) 1 wt.-%, (e) 3 wt.-%, and (f) 5 wt.-% of AMH-3.

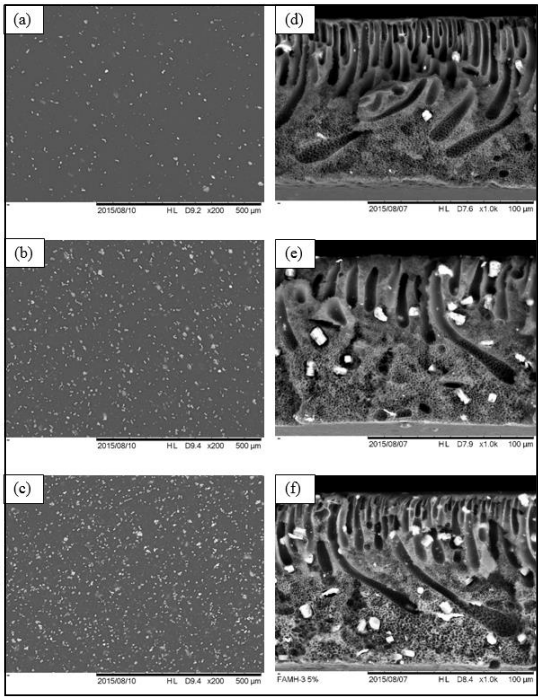

Fig. 5. Surface morphology of MMM with different loadings of functionalized AMH-3 at (a) 1 wt.-%, (b) 3 wt.-%, and (c) 5 wt.-%; and cross-section morphology with (d) 1 wt.-%, (e) 3 wt.-%, and (f) 5 wt.-% of functionalized AMH-3.

Figure 5 shows the surface and cross-sectional images of MMM incorporated with functionalized AMH-3. Similar to MMM of as-synthesized AMH-3, the surface morphologies of MMM with functionalized AMH-3 show good distribution and dispersion of AMH-3 fillers. No obvious particle agglomeration of functionalized AMH-3 is observed in the surface morphology.

Figure 6 illustrates the mapping of silicon in MMM for different loading of as-synthesized and functionalized AMH-3. In agreement with the SEM analysis, the uniform scattering of silicon element indicates good distribution and dispersion of the AMH-3 filler in the MMM. In summary, both as-synthesized and functionalized AMH-3 MMMs show similar surface and cross-sectional morphologies.

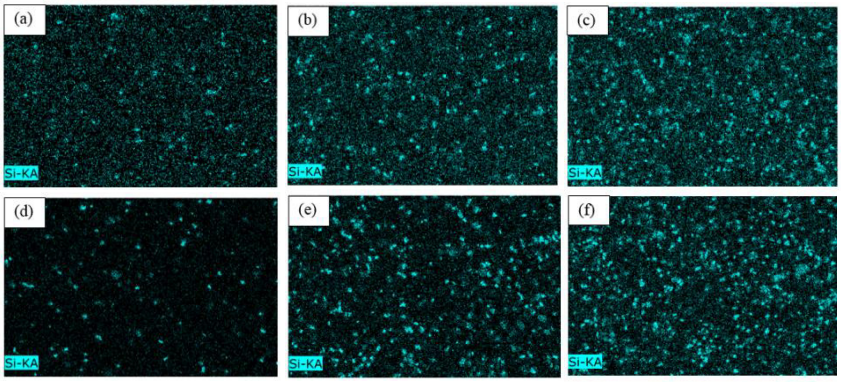

Figure 6. Element mapping of silicon for MMM incorporated with as-synthesized AMH-3 of (a) 1 wt.-%, (b) 3 wt.-%, (c) 5 wt.-% and functionalized AMH-3 of (e) 1 wt.-%, (f) 3 wt.-%, (g) 5 wt.-%

Contact angles of the membranes were measured in order to study the surface properties of the membranes. Images of water droplets on the membrane surface were captured by a computer controlled video capture system. The contact angle for each sample is listed in Table 1. MMMs incorporated with as-synthesized AMH-3 are more hydrophilic as the contact angles are smaller; whereas MMMs with functionalized AMH-3 showed greater hydrophobicity with larger contact angle. This proves that the modification of AMH-3 increases its hydrophobicity for better compatibility with PSf matrix which is hydrophobic in nature.

Figure 7 shows the weight loss curves of PSf membrane and selected MMMs. Generally, MMMs are expected to exhibit enhanced thermal stability by incorporation of inorganic fillers. Neat PSf membrane shows a substantial weight loss occurring at around 530°C. AMH-3 MMM also shows similar decomposition temperature with slight improvement of the thermal stability after functionalization. The residual mass of MMM with as-synthesized AMH-3 is the highest followed by the MMM with functionalized AMH-3, while the pure PSf membrane showed the lowest residual weight at 800°C. It can be assumed that the thermal stability of PSf is not changed to a great extent by the incorporation of as-synthesized and functionalized AMH-3.

Table 1: Contact angle of MMMs

Sample	Contact Angle (°)
Pure PSf	66.6
PSf/1wt% AMH-3	64.4
PSf/3wt% AMH-3	63.7
PSf/5wt% AMH-3	62.1
PSf/1wt% FAMH-3	68.0
PSf/3wt% FAMH-3	70.8
PSf/5wt% FAMH-3	83.5

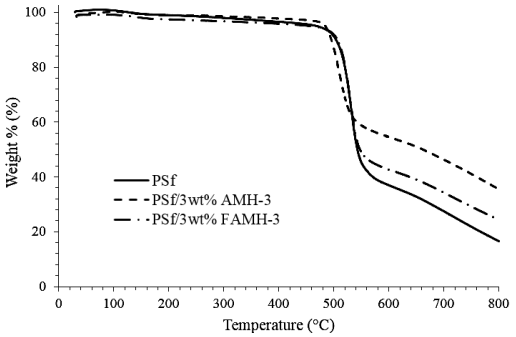

Figure 7. TGA curves of pristine PSf membrane and selected MMMs

4. Conclusion

AMH-3 layered silicate was successfully synthesized via hydrothermal synthesis and subsequently verified by FT-IR and XRD analysis. Surface modification of AMH-3 was carried out by proton exchange and swelling followed by functionalization via silane condensation method. The critical concentration of PSf in NMP solvent was determined by viscometric method as 23 wt.-%. MMMs were fabricated with 1, 3, 5 wt.-% of as-synthesized and functionalized AMH-3 in PSf matrix. The SEM analysis shows good distribution and dispersion of inorganic filler in MMMs with similar surface and the cross-sectional morphology for as-synthesized functionalized AMH-3. The functionalization of AMH-3 is found to improve the hydrophobicity of the AMH-3 and thus allow better adhesion and compatibility with PSf. Based on the TGA, incorporation of AMH-3 into MMMs show similar weight loss curves. The incorporation of as-synthesized and functionalized AMH-3 in PSf membrane is expected to enhance the gas separation performance of the membrane.

Acknowledgements

This work is financially supported by Universiti Teknologi PETRONAS (UTP) under FYP Cost Centre No. 015210-003 and URIF Grant No.0153AA-B27 for 2014-2016. The technical support provided by CO_2 Management Mission Oriented Research (MOR) is duly acknowledged.

References

[1] A. L. Ahmad, Z. A. Jawad, S. C. Low, and S. H. S. Zein, "Prospect of mixed matrix membrane towards CO2 separation," Journal of Membrane Science & Technology, 2012.
[2] O. Bakhtiari and N. Sadeghi, "The Formed Voids around the Filler Particles Impact on the Mixed Matrix Membranes' Gas Permeability," International Journal of Chemical Engineering and Applications vol. 5, pp. 198-203, 2014.
[3] M. Tsapatsis, H. K. Jeong, and S. Nair, "Layered silicate material and applications of layered materials with porous layers," ed: Google Patents, 2005.
[4] H.-K. Jeong, S. Nair, T. Vogt, L. C. Dickinson, and M. Tsapatsis, "A highly crystalline layered silicate with three-dimensionally microporous layers," Nat Mater, vol. 2, pp. 53-58, 01//print 2003.
[5] S. Choi, J. Coronas, Z. Lai, D. Yust, F. Onorato, and M. Tsapatsis, "Fabrication and gas separation properties of polybenzimidazole (PBI)/nanoporous silicates hybrid membranes," Journal of Membrane Science, vol. 316, pp. 145-152, 5/15/ 2008.
[6] W.-g. Kim, J. S. Lee, D. G. Bucknall, W. J. Koros, and S. Nair, "Nanoporous layered silicate AMH-3/cellulose acetate nanocomposite membranes for gas separations," Journal of Membrane Science, vol. 441, pp. 129-136, 8/15/ 2013.
[7] M. Rezakazemi, A. Ebadi Amooghin, M. M. Montazer-Rahmati, A. F. Ismail, and T. Matsuura, "State-of-the-art membrane based CO2 separation using mixed matrix membranes (MMMs): An overview on current status and future directions," Progress in Polymer Science, vol. 39, pp. 817-861, 5// 2014.
[8] N. Takahashi and K. Kuroda, "Materials design of layered silicates through covalent modification of interlayer surfaces," Journal of Materials Chemistry, vol. 21, pp. 14336-14353, 2011.
[9] S. Choi, J. Coronas, J. A. Sheffel, E. Jordan, W. Oh, S. Nair, et al., "Layered silicate by proton exchange and swelling of AMH-3," Microporous and Mesoporous Materials, vol. 115, pp. 75-84, 10/1/ 2008.
[10] H. Hachisuka and K. Ikeda, "Polysulfone semipermeable membrane and method of manufacturing the same," ed: Google Patents, 1999.
[11] J. Ahn, W.-J. Chung, I. Pinnau, and M. D. Guiver, "Polysulfone/silica nanoparticle mixed-matrix membranes for gas separation," Journal of Membrane Science, vol. 314, pp. 123-133, 4/30/ 2008.
[12] W. J. Koros, D. Q. Vu, R. Mahajan, and S. J. Miller, "Mixed matrix membranes capable of separating carbon dioxide from mixtures including carbon dioxide and methane, and processes for purifying methane using the membranes, are disclosed. The membranes are polymer membranes with a," ed: Google Patents, 2003.
[13] A. M. W. Hillock, S. J. Miller, and W. J. Koros, "Crosslinked mixed matrix membranes for the purification of natural gas: Effects of sieve surface modification," Journal of Membrane Science, vol. 314, pp. 193-199, 4/30/ 2008.
[14] S. A. McKelvey and W. J. Koros, "Phase separation, vitrification, and the manifestation of macrovoids in polymeric asymmetric membranes," Journal of Membrane Science, vol. 112, pp. 29-39, 4/3/ 1996.
[15] N. Peng, T.-S. Chung, and K. Y. Wang, "Macrovoid evolution and critical factors to form macrovoid-free hollow fiber membranes," Journal of Membrane Science, vol. 318, pp. 363-372, 6/20/ 2008.
[16] T. S. Chung, S. K. Teoh, and X. Hu, "Formation of ultrathin high-performance polyethersulfone hollow-fiber membranes," Journal of membrane science, vol. 133, pp. 161-175, 1997.
[17] S. Nair, Z. Chowdhuri, I. Peral, D. A. Neumann, L. C. Dickinson, G. Tompsett, et al., "Translational dynamics of water in a nanoporous layered silicate," Physical Review B, vol. 71, p. 104301, 2005.
[18] B. Morrow and I. Gay, "Infrared and NMR characterization of the silica surface," Surfactant Science Series, pp. 9-34, 2000.
[19] W.-g. Kim, S. Choi, and S. Nair, "Swelling, Functionalization, and Structural Changes of the Nanoporous Layered Silicates AMH-3 and MCM-22," Langmuir, vol. 27, pp. 7892-7901, 2011/06/21 2011.
[20] K. S. W. Sing, D. H. Everett, R. A. W. Haul, L. Moscou, R. A. Pierotti, J. RouqueroL, et al., "Reporting physisorption data for gas/solid systems, with special reference to the determination of surface area and porosity (recommendations 1984)," Pure and applied chemistry, vol. 57, pp. 603-619, 1985.
[21] P. K. Jal, S. Patel, and B. K. Mishra, "Chemical modification of silica surface by immobilization of functional groups for extractive concentration of metal ions," Talanta, vol. 62, pp. 1005-1028, 4/19/ 2004.